Extended Abstracts of the 16th (1984 International) Conference on Solid State Devices and Materials, Kobe, 1984, pp. 407-411

Field Effect Studies on MIS Structures of p-Type $Hg_{0.8}Cd_{0.2}Te$ Thin Films

A.L. Dawar, K.V. Ferdinand, C. Jagadish, Anil Kumar and P.C. Mathur

Department of Physics and Astrophysics

University of Delhi, Delhi - 110 007, India

D.C. conductivity and Hall coefficient studies were made on MIS structures of $Hg_{0.8}Cd_{0.2}Te$ thin films as function of gate field and temperature (77-400 K). Decrease and increase in Hall coefficient and Hall mobility with negative and positive gate fields have been attributed to the accumulation and depletion of majority carriers. The mobility-temperature data have been analysed in terms of different scattering mechanisms.

Introduction:

Metal-insulator-semiconductor (MIS) structures fabricated from narrow gap semiconductors are becoming increasingly important in monolithic infrared imaging application[1,2]. A detailed study of the electrical transport properties of thin films of MIS structures can provide valuable information needed for exploitation of MOS technology for device fabrication.

$Hg_{1-x}Cd_xTe$ is an important intrinsic semiconductor for the fabrication of photovoltaic and photoconductive infrared detectors. The alloys with composition x=0.20 are particularly important for the devices 8-14 μm radiation in the atmospheric window region[3-6].

In the present work, the effect of gate field on Hall coefficient and d.c. conductivity has been studied on MIS structures of p-$Hg_{0.8}Cd_{0.2}Te$ films grown on mica and glass at various temperatures. The observed results have been interpreted in terms of accumulation and depletion of charge carriers at the insulator-semiconductor interface upon the application of gate field.

Experimental Details:

$Hg_{0.8}Cd_{0.2}Te$ films of 0.7 μm thick and rectangular in shape (20x4 mm^2) were grown by flash evaporation technique on to the freshly cleaved mica and ultrasonically cleaned glass subtrates kept at 100°C using tantalum masks under a vacuum $\sim 5\times10^{-6}$ Torr. The growth rate was $\sim$ 30 A°/sec. Electrical contacts were made by evaporation of high purity Indium on to the films under vacuum using tantalum masks. The ohmic nature of the contacts was confirmed throughout the temperature range by their linear I-V characteristics. The gate contacts were obtained by evaporating Indium at the back of the substrates. X-ray diffraction studies were made using Philips X-ray diffractometer (model No. 1130/00) employing Cu K_α radiation. Composition studies were made using Electron Probe Micro Analyser (Philips SEM 505 + EDAX + WDX). The d.c. conductivity and Hall coefficient studies were made as discussed in one of our earlier papers[7].

Results and Discussion:

1. X-ray diffraction studies:

Diffractometer spectra for the films and for $Hg_{0.8}Cd_{0.2}Te$ powder are shown in Fig. 1. The spectrum of the powder is seen to exhibit sharp peaks at 2 θ equal to 23.8°, 39.4°, 46.5° and 57° which corresponds to diffraction from (111), (220), (311) and (400) planes of the cubic phase respectively. The lattice constant calculated from the 'd' values of the peaks was in good agreement with the reported data[3]. Films grown on glass substrates showed only one peak at 2 θ equal to 23.8° which corresponds to (111) plane of the cubic phase and the other planes (220), (311) and (400) were absent in the films. The (111) direction is the close packing direction of the zinc blend structure.

The grain size ' l ' is calculated from Scherrer formula[8]

$$l = \lambda / D\cos\theta$$

where D is the full width at half maximum of the peak, λ is the wavelength of the X-rays. The value of ' l ' calculated for the as grown films is 560 A°.

Electron diffraction studies also confirmed the polycrystalline nature of the films grown on glass.

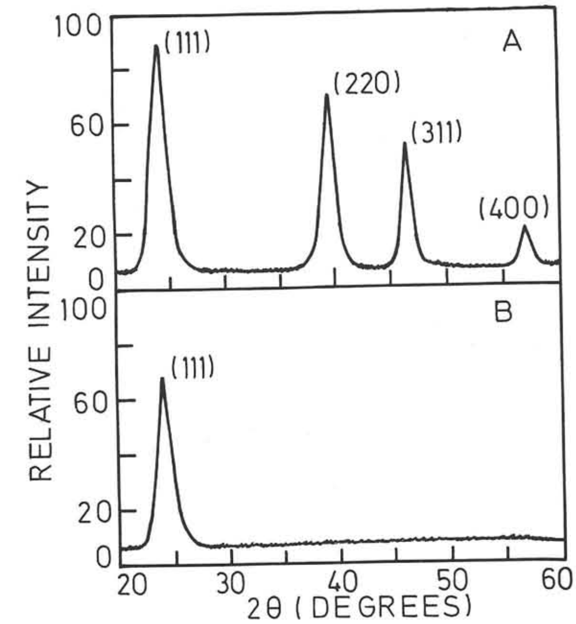

Fig. 1. X-ray diffraction spectra (a) bulk $Hg_{0.8}Cd_{0.2}Te$ powder (b) as grown film.

2. Composition Analysis:

EPMA studies were made on the films and on the starting material to know the actual composition. Energy dispersive system was employed to know the various elements present in the bulk and in the films and to determine their concentration. Composition analysis with ZAF correction is shown in Table-I. It can be observed from Table-I only Hg, Cd and Te were present in both bulk and films. It can be further observed from Table I that the films were containing little excess of Te because of which the films showed p-type conductivity.

Table-I. Composition Analysis

Ele-ment	Amount taken in at. %	Bulk at. %	Film at%
Hg	40	39.84	39.71
Cd	10	9.92	9.89
Te	50	50.24	50.40

Electrical Properties

The variation of Hall coefficient R_H as a function of temperature (log R_H vs. 1000/T) in the temperature range 77-400 K, for a typical MIS structure at various gate fields is shown in Fig. 2. It is observed from this figure that in the absence of any gate field, the value of R_H remains practically constant in the low temperature region 77-200 K, showing the behaviour of a typical degenerate semiconductor. The value of R_H is found to decrease with the rise of temperature above 200 K. The decrease in R_H at higher temperatures can be attributed to the fact that a contribution due to grain boundary potential starts above 200K. It can also be observed from Fig. 2 that the value of R_H at any temperature decreases with the increase of negative gate field, while the effect of positive gate field is to increase the value R_H. This is because of the fact that in the case of p-type films when a negative gate voltage is applied to the metal plate (i.e. negative gate field), the top of the valence band bends upward and comes closer to the Fermi level. This band bending causes an accumulation of majority carriers (holes) at the interface. Since the film is thin enough, the carriers which are accumulated at the interface are redistributed in the whole film and so a decrease in the value of R_H is observed. On the other hand, the effect of a positive gate field is to bend the bands downwards and to deplete the majority carriers, thereby increasing the value of R_H.

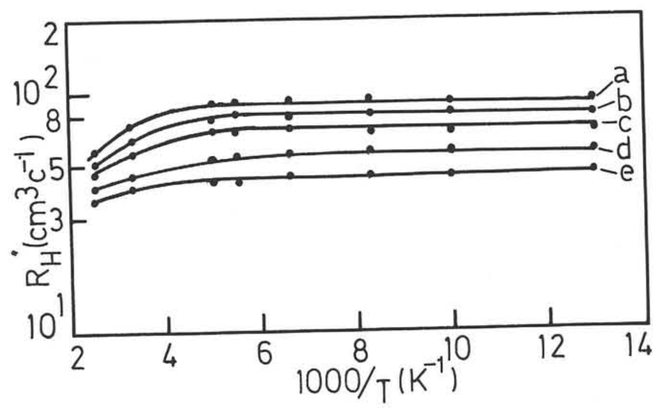

Fig. 2. Variation of Hall coefficient with temperature (log R_H vs 1000/T).
(a) 7.5×10^5 V/cm (b) 3.75×10^5 V/cm
(c) Zero (d) -3.75×10^5 V/cm
(e) -7.50×10^5 V/cm

It can be further observed from Fig. 2 that the temperature at which R_H starts decreasing is changing with the applied gate field suggesting that the onset of the contribution of grain boundary scattering depends on the applied gate field.

The variation of Hall mobility, μ_H as a function of temperature (log μ_H vs. 1000/T) at various gate fields is shown in Fig. 3. It can be observed from Fig. 3 that the value of the Hall mobility at any temperature decrease with negative gate field, while effect of positive gate field is to increase the mobility. This type of variation of the mobility with various gate fields can be due to the fact that the gate field causes a change in free carrier concentration. It can also be seen from this figure that at any gate field, the value of μ_H increases with the increase of the temperature. The increase in μ_H with temperature in the low temperature region (77-200 K) is slow whereas the increase is faster in the high temperature region. This can be attributed to the thermally assisted tunneling of the carriers through grain boundaries and thermionic emission of the carriers over the grain boundaries in the low and high temperature regions respectively.

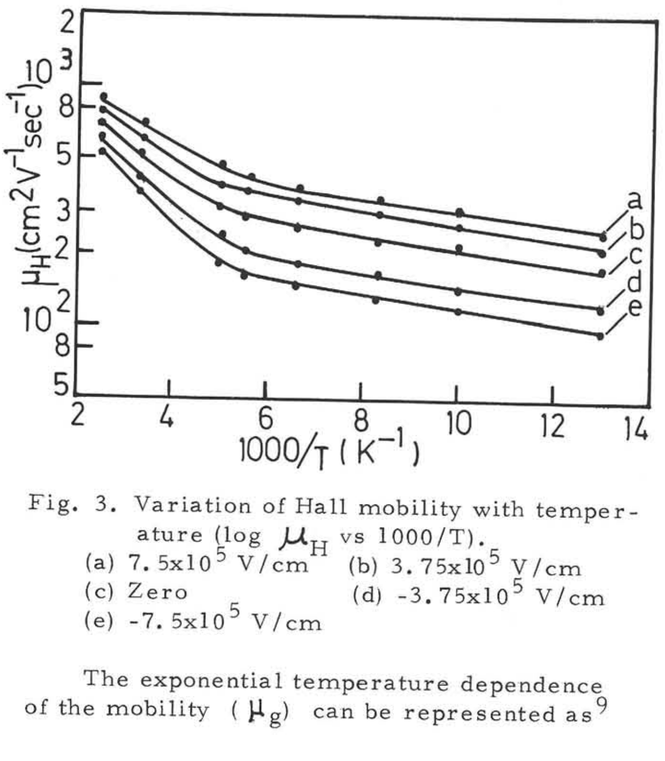

Fig. 3. Variation of Hall mobility with temperature (log μ_H vs 1000/T).
(a) 7.5×10^5 V/cm (b) 3.75×10^5 V/cm
(c) Zero (d) -3.75×10^5 V/cm
(e) -7.5×10^5 V/cm

The exponential temperature dependence of the mobility (μ_g) can be represented as[9]

$$\mu_g = \mu_0 / T^{1/2} \exp(-e\phi_b/KT) \quad (1)$$

where $e\phi_b$ is the grain boundary barrier potential. The term μ_0 depends on the average grain size 'l' by the relation

$$\mu_0 = el\left(\frac{8}{\beta^2 \pi K m}\right)^{1/2}$$

where β is a numerical constant, m is the effective mass of the charge carriers, 'e' is the charge of the carriers and K is the Boltzmann constant.

The grain boundary barrier potential ($e\phi_b$) has been estimated at various gate fields using the relation (1) and the values of '$e\phi_b$' thus calculated are shown in Table -II. It can be seen from this table that the values of '$e\phi_b$' increases with the increase of negative gate field, where as the effect of positive gate field is to decrease the value of '$e\phi_b$'. The increase in '$e\phi_b$' suggests that the contribution of grain boundary scattering increases with the increase of negative gate field. This explains the observed decrease in μ_H with negative gate field. In addition to the grain boundary scattering contribution, there may be a significant effect of surface states and their occupation on the variation of mobility with temperature. In order to see the effects of surface states, the data have been analysed in detail in the following manner.

Table-II. Variation of $e\phi_b$ with gate field

S.No.	Gate field V/cm	Grain boundary barrier potential $e\phi_b$ in meV
a.	7.50×10^5	21.30
b.	3.75×10^5	24.90
c.	zero	28.24
d.	-3.75×10^5	32.67
e.	-7.50×10^5	37.15

The d.c. conductivity have been used to calculate the effective field effect mobility μ_{FE} as a function of temperature. Total charge induced at the interface (Q_s) as a function of applied gate field has been calculated using the relation[10]

$$Q_s = \epsilon_0 \epsilon_i V_p / t \quad (2)$$

where V_p is the field electrode potential, 't' is the thickness of the insulator, ϵ_0 is the permittivity of free space and ϵ_i is the relative permittivity of the insulator.

The value of the effective field effect mobility μ_{FE} has been thus computed using the relation[11, 12]

$$\mu_{FE} = d(\Delta\sigma) / dQ_s \quad (3)$$

where $\Delta\sigma$ is the observed change in surface conductance, when gate field is applied. The value of $\Delta\sigma$ has been calculated using the relation[11, 12]

$$d.\ \sigma_g = d.\ \sigma_0 + \Delta\sigma \quad (4)$$

where σ_g is the average conductivity actually measured at a given gate field, σ_0 is the value of the conductivity at zero gate field and 'd' is the thickness of the film.

The variation of effective field effect mobility with temperature (log μ_{FE} vs log T) is shown in Fig. 4. It can be observed from this fig. that the μ_{FE} is increasing with the increase of temperature in accordance with the relation $\mu_{FE} \propto T^{\delta}$. The value of δ calculated from the temperature variation of μ_{FE} is found to be ~ 0.76, indicating that charged fast interface traps and surface states charge scattering are the dominant scattering mechanism[13,14]. This temperature variation of μ_{FE} may also be due to the change in

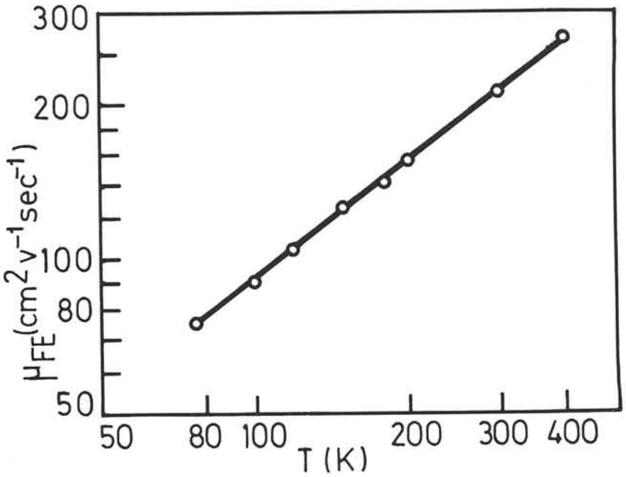

Fig. 4. Variation of effective field effect mobility with temperature ('log μ_{FE} vs. log T).

occupancy of surface states with temperature. To study this effect, the value of excess charge in the space charge region $e\,|\Delta p|$ was calculated using the relation[11,12]

$$e|\Delta p| = \left| \frac{(\Delta\sigma)^2}{\Delta(R_H \sigma^{-2})} \right| \tag{5}$$

where $\Delta\sigma$ the surface conductance is calculated using the relation (4) and $\Delta(R_H\sigma^{-2})$ is calculated using the relation

$$d.R_{Hg}\sigma_g^{-2} = d.R_{Ho}\sigma_o^{-2} + \Delta(R_{Hg}\sigma^{-2}) \tag{6}$$

where R_{Ho} is the value of Hall coefficient measured at zero gate field and R_{Hg} is the value measured at any given field. The values of $e|\Delta p|$ thus calculated at various temperatures are practically constant with temperature. This suggests that there is no significant contribution of the change in occupancy of the surface states and traps with temperature, to the temperature dependence of μ_{FE}. The above analysis shows that there is a considerable contribution of grain boundaries as well as surface states to the conduction mechanism in these MIS structures.

Acknowledgements:

Authors would like to thank Prof. S. Varadarajan and Mr. P.C. Padmakshan. for providing the use of X-ray diffraction equipment. One of the authors (C.J.) gratefully acknowledges the financial assistance from the Council of Scientific and Industrial Research, New Delhi.

References

1. J.T. Longo, D.T. Cheung, A.M. Andrews, C.C. Wang and J.M. Tracy, IEEE Trans. Electron Devices ED-25, 213 (1978).

2. P.H. Zimmerman, M.E. Mathews and D. E. Joslin., J. Appl. Phys., 50, 5815 (1979).

3. R. Dornhaus and G. Nimtz., Solid State Physics, Springer Tracts in Modern Physics (Springer-Verlag, Berlin, 1976) vol. 78.

4. D. Long and J.L. Schmit, Semiconductors and Semi-metals, edited by R.K. Willardson and A.C. Beer (Academic Press, New' York, 1970), vol. 5, p. 175.

5. D.L. Carter, N.A. Kinchand and D.D. Buss. The Physics of Semi-metals and Narrow gap semiconductors, edited by D.L. Carter, (Pergamon Press, Dallas, 1970), p. 273.

6. T.C. Harman and I. Melngailis, Applied Solid State Science, edited by R. Wolfe (Academic Press, New York, 1974), vol. 4.

7. A.L. Dawar, C. Jagadish, K.V. Ferdinand, Suranjan Pal, Anil Kumar and P.C. Mathur, Proceedings of 6th European Conference on Surface Science held at York, U.K., April, 1984. Surface Science (In Press).

8. L.I. Maissel and R. Glang, Hand Book of Thin Film Technology, McGraw Hill Book Co., New York (1970).

9. J.W. Ortan, B. Goldsmith, M.J. Powell and A.J. Chapman, Appl. Phys. Lett., 37, 557 (1980).

10. A. Many, Y. Goldstein and N.B. Grover, Semiconductor Surfaces, North Holland Publishing Co., Amsterdam (1965).

11. J.N. Zemel, Phys. Rev., 112, 762 (1958).

12. A. Amith, J. Phys. Chem. Solids, 14, 271 (1960).

13. M.E. Sproul and A.G. Nassibian, J. Appl. Phys., 46, 1255 (1975).

14. C.T. Sah, T.H. Ning and L.L. Tschopp, Surface Science, 32, 561 (1972).